의학석사 학위논문

Relationship between adverse plaque characteristics and wall shear stress assessed by computational fluid dynamics

전산 유체 역학에 의해 평가된 벽 전단 응력과 유해한 플라크 특성 사이의 관계

2018년 2월

서울대학교 대학원
의학과 내과학 전공
기유정

Abstract

Relationship between adverse plaque characteristics and wall shear stress assessed by computational fluid dynamics

You Jeong Ki

Department of Internal Medicine

Seoul National University College of Medicine

Background: Computational fluid dynamics (CFD) is novel noninvasive technology that can provide information of coronary hemodynamics. This study attempted to determine whether the wall shear stress (WSS) evaluated by CFD is related to the adverse plaque characteristics (APC).

Methods: We retrospectively enrolled 296 lesions in 143 subjects (mean age 66.7 ± 11.8, male 80.4%) who underwent coronary computed tomography angiography. Hemodynamic parameters including flow, pressure, pressure drop over length (pressure gradient), non-invasive fractional flow reserve from coronary computed tomography angiography and WSS were computed from CFD analysis. The presence of APC, which was defined as low density plaque, positive remodeling, napkin ring sign and spotty calcification, was assessed in the minimal lumen area segment.

Results: Plaque with any of high risk features were found in 147 of 296 lesions (49.7%) and the most common feature was low density plaque (n = 82, 27.7%). The plaques exposed to the highest WSS tertile had a significantly greater proportion of high risk plaques. In the receiver operating characteristic curve analysis, the cut off value of WSS for the prediction of any high risk feature plaque is 161. The addition of high WSS (hyperemic WSS ≥ 161 dyne/cm^2) to % diameter stenosis improved the discrimination and reclassification of high risk plaques (area under the curves from 0.648 to 0.673, $P < 0.001$; category free net reclassification index 0.406, $P < 0.001$; integrated discrimination index 0.021, $P = 0.010$). The incremental value of high WSS over % diameter stenosis was observed for each feature of APC except for spotty calcification.

Conclusions: Hemodynamics of computed tomography derived computational models is feasible and non-invasive technology, and may be useful in assessing adverse plaque.

Keywords: wall shear stress, computational fluid dynamics, plaque, coronary artery disease, coronary computed tomography angiography.

Student Number: 2016-21910

Contents

Introduction

There are three main causes of coronary thrombosis, which are rupture, erosion and calcified nodule. Above all, plaque rupture is the most crucial mechanism leading to acute coronary syndrome.(1, 2) Rupture of the plaque's cap triggers contact between coagulation factors in the blood and tissue factor and produces thrombus.(1) Histologic studies have shown that easily ruptured plaques have rich lipid core, thin fibrous cap, and spotty calcification.(1) But prediction of plaque rupture is still difficult.

The risk of plaque rupture is dependent on both plaque vulnerability (intrinsic component) and rupture triggers (extrinsic stress).(3) When the plaque stress becomes exceed plaque strength, a plaque rupture may be occurred. Wall shear stress (WSS) is one of the important extrinsic factors in the process of plaque rupture. WSS is defined as a tangential force resulting from the friction between the blood flow and the vessel endothelium.(4)

Previous studies have shown that lower arterial WSS (< 4 dyne/cm2) is responsible for the atherosclerosis and sub intimal thickening, whereas physiological or elevated arterial WSS (> 15 dyne/cm2) is associated with atheroprotective endothelial function.(5) Despite clinical importance of WSS, its association between very high WSS and adverse plaque characteristics (APC) has not been well studied, yet. There are several studies dealing with risk of higher WSS.(6) In a recent coronary computed tomography angiography (CCTA) based

computational fluid dynamics (CFD) study, the plaque exposed higher WSS had a tendency of association with high risk plaque.(6, 7)

Hemodynamic factors are thought to be used for localization of cardiovascular disease in the area of complex blood flow in the coronary arteries.(8) Recent progress of CCTA and CFD enables measure hemodynamic forces effect on plaques and facilitate quantification of hemodynamic parameters including blood velocity, pressure, pressure drop over length (pressure gradient), fractional flow reserve (FFR) and WSS.(9-11) The value of CFD has been validated in many small studies and is being used to evaluate coronary hemodynamics.(6, 10)

There have been several papers on the relationship between APC and WSS, but only in a small number of patients.(6) This study was performed to investigate the association between WSS and APC using CCTA based CFD analysis of coronary hemodynamics in a larger number of subjects.

Materials and methods

Study population

The population of this study included 2 different trials. First, the Evaluation of FFR, WSS, and total plaque force Using CCTA is a trial to assess the feasibility of computed tomography-derived hemodynamic parameters. (NCT01857687) From May 2013 through May 2014, stable patients with suspected or known coronary artery disease were enrolled. Second, Exploring the MEchanism of Plaque Rupture in Acute Coronary Syndrome Using Coronary CT Angiography and computationaL Fluid Dynamic (EMERALD) trial is a multinational, multicenter study. (NCT02374775) The patients who presented with myocardial infarction and underwent coronary CT angiography from 1 month to 2 year prior to the event were retrospectively searched. Except for poor CT images, which unable to be reconstructed in 3 dimensional, 61 were enrolled from the first trial and 82 were enrolled from the second trial. A total of 143 patients were enrolled. The study protocol was approved by the institutional review boards of each hospital and was implemented in accordance with the Declaration of Helsinki.

Image acquisition of CCTA and CFD analysis

The CCTA images were obtained in accordance with the Society of Cardiovascular Computed Tomography Guidelines on performance of CCTA, with 64 or higher

detector row scanner platforms.(12) Oral beta blockers were administered for any subjects with a heart rate ≥ 65 beats/min. Immediately before the CCTA acquisition, 0.2 mg of sublingual nitroglycerin was administered for coronary vasodilatation. All CCTA data were analyzed by a single core laboratory (HeartFlow, Redwood City, California, USA) in a blinded manner. The finite element method has been used for solving the equations governing coronary blood flow. A Newtonian constitutive model for viscosity was used for this study. It is generally accepted method for evaluation of blood flow in large arteries.(8) Allometric scaling law shows relationship between metabolic rate and body mass. Baseline coronary artery flow is proportional to myocardial mass and microvascular resistance is inversely proportional to vessel area. Through this way, myocardial microcirculatory resistance was determined.(9, 13, 14) Hemodynamic parameters including flow, pressure, pressure drop over length (pressure gradient), non-invasive FFR from CCTA (FFR_{CT}) and WSS were computed from CFD analysis. (Figure 1) WSS is the tangential stress due to the friction of blood flow on the endothelial surface of the arterial wall. WSS was defined as the product of shear rate and blood viscosity. The shear rate is the spatial gradient of the blood velocity in s^{-1}. The WSS can be calculated by following formula:

$$\text{Wall shear rate} = \frac{\text{difference in velocity } (\text{m}S^{-1})}{\text{distance (m)}}$$

$$\text{Wall shear stress} = \text{wall shear rate} \times \text{viscosity} = \frac{4\mu Q}{\pi R^3}$$

where μ is the blood viscosity, Q is the blood flow, and R is the vessel radius. FFR_{CT} is calculated by ratio of mean downstream coronary pressure divided by the upstream pressure. Hyperemic conditions were regulated by reducing the microcirculatory resistances in consistent with the effects of adenosine. To understand the regional characteristics in stenotic lesions, each stenotic lesion was subdivided into upstream, minimal lumen area (MLA) and downstream segments with respect to the location of MLA.

Analysis of coronary plaque characteristics

Coronary lesions were defined as plaques of an area ≥ 1 mm^2 within and/or adjacent to the vessel lumen, which could be clearly distinguished from the lumen and surrounding tissue. For each coronary lesion, the presence of APC, which were defined as low density plaque, positive remodeling, napkin ring sign and spotty calcification, was assessed in the MLA segment. This interpretation was performed by an independent observer blinded to the clinical data and CFD results, based on previous studies. Briefly, plaque density was assessed using an automated software program that can analyze each pixel within the plaque. The low density plaque was defined as the plaque density with lower than 30 Hounsfield units (HU). To identify the presence of low density plaque, a region of interest was placed on at least five randomly selected points within each plaque, and the mean value was defined as the plaque density. The remodeling index was calculated as the outer

vessel diameter at the site of maximal stenosis divided by the reference diameter. A remodeling index threshold of ≥ 1.10 was used to define positive remodeling. The napkin ring sign was defined as a ring like attenuation pattern of the coronary plaque with peripheral high attenuation tissue surrounding a central lower attenuation portion, which has been increasingly recognized as a key feature of high risk plaques. Spotty calcification was defined as a small (< 3 mm), dense (> 130 HU) plaque component surrounded by non-calcified tissue of the plaque. A plaque with at least one feature of APC was defined as a high risk plaque. The WSS averaged over the MLA segment was used to assess the association between APC and WSS.

Statistical analysis

Categorical and continuous variables are given as counts (percentages) and mean ± standard deviation. Mean values of hemodynamic parameters were compared using the independent t-sample test To compare APC across WSS tertiles, we used the χ^2 test for categorical variables. And the mean values between the three groups were compared by analysis of variance followed by Tukey's honest significant difference test among different groups. Pearson's correlation coefficients were calculated to determine the relationship among hemodynamic parameters associated to plaque stress. Lesion based bivariate and multivariate analyses were performed using the generalized estimating equation approach to account for several lesions within the

same subject. The association between WSS and high risk plaques was modelled with logistic regression, and non-linearity was explored using multivariable fractional polynomials. We constructed receiver operating characteristic curves and determined their area under the curves (AUC) to assess the ability of the variables of interest to discriminate plaques with APC. The incremental value of WSS in discriminating APC was explored by constructing two models, one with luminal narrowing alone and the other with luminal narrowing plus high WSS. The AUC in each model was calculated and compared for statistical significance. The category free net reclassification index and integrated discrimination improvement analysis were performed. All statistical analyses were conducted with SPSS V.22 (IBM SPSS Statistics, Chicago, Illinois, USA) and STATA Release 12.0 (Stata, College Station, TX, USA). A two-sided P value < 0.05 was considered as significant.

Results

Baseline characteristics

Baseline characteristics of the study subjects are listed in Table 1. A total of 143 patients with 296 lesions were enrolled (mean age 66.7 ± 11.8, male 80.4%). There were 296 stenotic lesions and their distributions were as follows: left main coronary artery or left anterior descending (n = 167), left circumflex (n = 48) and right coronary artery (n = 81). The MLA and % diameter stenosis (DS) by CCTA were 2.6 ± 1.5 mm^2 and 48.4 ± 15.8%, respectively. Plaques with any of high risk features were found in 147 of 296 stenotic lesions (n = 147, 49.7%) and the most common feature was low density plaque (n = 82, 27.7%).

Distribution of anatomic variables and hemodynamic parameters

Comparison of anatomic variables and hemodynamic parameters between adverse plaque and non-adverse plaque are shown in Table 2. In lesions with APC, mean % DS was higher than non APC lesion. Lesion length and location of lesion were similar between two groups. Delta pressure, pressure gradient, WSS and delta FFR_{CT} were higher in APC lesion than non APC lesion.

Determinants of WSS

There was a strong positive relation between average WSS and pressure gradient across at hyperemic condition ($r = 0.935$, $P < 0.001$) and resting condition ($r = 0.912$, $P < 0.001$). By multivariate analysis, delta pressure, lesion location, MLA and lesion length were independent determinants for the magnitude of WSS at hyperemic and resting conditions. (Table 3)

WSS and APC

Characteristics of coronary plaques stratified by the tertiles of hyperemic WSS are shown in Table 4. Tertiles of mean WSS were divided into low (range < 124.3 dyne/cm^2), intermediate (range 124.3-212.7 dyne/cm^2) and high groups (range > 212.7 dyne/cm^2). The plaques exposed to the highest WSS tertile had a significantly greater proportion of high risk plaques. Specifically, low density plaque, positive remodeling or napkin ring sign was more prevalent in the highest WSS tertile. But, spotty calcification was not showed that tendency. Similar relationships could be found in resting WSS. (Table 5)

When the logistic regression model with multivariable fractional polynomials was used to explore the association between hyperemic WSS and high risk plaques, the odds ratio (OR) of plaque with any of high risk features increased as the value of hyperemic WSS increased. Notably, we found that the OR of plaque with any of high risk features also increased when the value of hyperemic WSS decreased below 40 dyne/cm^2. (Figure 2)

In the receiver operating characteristic curve analysis, the cut off values of WSS for the prediction of APC are shown in Table 6. The cut off value of hyperemic WSS for the prediction of plaque with any of high risk features was 161 and 43 at hyperemic and resting condition, respectively.

The association of % DS with plaque with any of high risk features was reflected by the AUC (0.648, $P < 0.001$). Compared with the baseline model of % DS alone, the receiver operating characteristic curve showed further discriminatory value for predicting high risk plaque when high hyperemic WSS (hyperemic WSS ≥ 161) was added (AUC from 0.648 to 0.673, $P < 0.001$; category free net reclassification index 0.406, $P < 0.001$; integrated discrimination index 0.021, $P = 0.010$) (Table 7). The incremental value of WSS over % DS was observed for each feature of APC except for spotty calcification.

Table 1. Baseline characteristics

Patients (n = 143)	
Age, years	66.7 ± 11.8
Female	28 (19.6%)
Body mass index, kg/m^2	24.5 ± 2.9
Height, cm	165.1 ± 8.7
Lesion characteristics (n = 296)	
Lesion locations	
Left main	8 (2.7%)
LAD	159 (53.7%)
LCx	48 (16.2%)
RCA	81 (27.4%)
Severity by CCTA	
Diameter stenosis, %	48.4 ± 15.8
Lesion length	18.2 ± 8.1
Minimal lumen area, mm2	2.6 ± 1.5
Distance from coronary ostium, mm	47.4 ± 22.8
Resting hemodynamic parameters	
Delta pressure, mmHg	2.4 ± 4.8
Average WSS, dyne/cm^2	42.9 ± 32.4
Proximal WSS, dyne/cm^2	51.0 ± 45.7

Distal WSS, dyne/cm^2	33.4 ± 28.0
Delta FFR_{CT}	0.03 ± 0.05
Adverse plaque characteristics	
Plaque with any of high risk features	147 (49.7%)
Low density plaque	82 (27.7%)
Positive remodeling	79 (26.6%)
Napkin ring sign	55 (18.6%)
Spotty calcification	69 (23.3%)

LAD, left anterior descending artery; LCx, left circumflex artery; RCA, right coronary artery; CCTA, coronary computed tomography angiography; WSS, wall shear stress; FFR, fractional flow reserve.

Table 2. Comparison of anatomic variables and hemodynamic parameters between adverse plaque and non-adverse plaque

Parameter	non APC (n = 149)	APC (n = 147)	*P*-value
Anatomic variables			
Diameter stenosis, %	44.2 ± 14.0	52.6 ± 16.5	< 0.001
Lesion length, mm	17.8 ± 8.1	18.6 ± 8.1	0.415
Minimal lumen area, mm^2	2.9 ± 1.6	2.3 ± 1.3	0.001
Distance from coronary ostium, mm	44.3 ± 21.9	40.3 ± 23.6	0.133
Resting			
Delta pressure, mmHg	1.3 ± 2.2	3.5 ± 6.2	< 0.001
Pressure gradient, mmHg/cm	1.03 ± 1.10	2.22 ± 3.11	< 0.001
Proximal pressure gradient, mmHg/cm	1.32 ± 1.89	2.85 ± 4.57	< 0.001
Distal pressure gradient, mmHg/cm	0.76 ± 0.83	1.58 ± 2.37	< 0.001
Average WSS, dyne/cm2	33.6 ± 19.5	52.3 ± 39.5	< 0.001
Proximal WSS, dyne/cm2	39.9 ± 30.6	62.1 ± 54.8	< 0.001

Distal WSS, dyne/cm2	26.1 ± 16.6	40.8 ± 34.6	< 0.001
Delta FFR_{CT}	0.01 ± 0.02	0.04 ± 0.07	< 0.001

APC, adverse plaque characteristics; WSS, wall shear stress; FFR, fractional flow reserve.

Table 3. Anatomic and hemodynamic determinants of wall shear stress

Parameter	β	95% CI	*P*-value
Hyperemia			
Delta pressure, mmHg	4.699	2.993 to 6.406	< 0.001
Distance from coronary ostium, per 1mm	-1.556	-1.958 to -1.154	< 0.001
MLA, per 0.1 mm^2	-0.891	-1.505 to -0.277	0.004
Lesion length, per 1mm	-2.303	-3.410 to -1.197	< 0.001
Resting			
Delta pressure, mmHg	4.299	3.135 to 5.462	< 0.001
Distance from coronary ostium, per 1mm	-0.286	-0.392 to -0.179	< 0.001
MLA, per 0.1 mm^2	-0.438	-0.581 to -0.296	< 0.001
Lesion length, per 1mm	-0.632	-0.909 to -0.356	< 0.001

CI, confidence interval; MLA, minimal lumen area.

Table 4. Adverse plaque characteristics according to tertiles of hyperemic WSS

	Low (n=99) WSS < 124.3	Intermediate (n=98) WSS 124.3-212.7	High (n=99) WSS > 212.7	*P*-value
Plaque with any of high risk features	36 (36.4%)	48 (49%)	63 (63.6%)	0.001
Low plaque density	19 (19.2%)	26(26.5%)	37 (37.4%)	0.016
Positive remodeling	14 (14.1%)	21 (21.4%)	44 (44.4%)	< 0.001
Napkin ring sign	11 (11.1%)	12 (12.2%)	32 (32.3%)	< 0.001
Spotty calcification	25 (25.3%)	19 (19.4%)	25 (25.3%)	0.532

WSS, wall shear stress

Table 5. Adverse plaque characteristics according to tertiles of resting WSS

	Low (n = 97) WSS < 25	**Intermediate (n = 99) WSS 25-45**	**High (n = 99) WSS > 45**	***P*-value**
Plaque with any of high risk features	37 (38.1%)	42 (42.4%)	68 (68.7%)	< 0.001
Low plaque density	30 (30.9%)	29 (29.3%)	48 (48.5%)	0.008
Positive remodeling	13 (13.4%)	22 (22.2%)	44 (44.4%)	< 0.001
Napkin ring sign	9 (9.3%)	14 (14.1%)	32 (32.3%)	< 0.001
Spotty calcification	22 (22.7%)	18 (18.2%)	29 (29.3%)	0.178

WSS, wall shear stress

Table 6. Cut off values of wall shear stress for the prediction of adverse plaque characteristics

Parameters	COV	AUC	CI	*P*	Sen	Spe
Hyperemia						
Plaque with any of high risk features	161	0.636	0.574-0.699	< 0.001	0.612	0.591
Low plaque density	184	0.600	0.529-0.672	0.008	0.549	0.621
Positive remodeling	198	0.686	0.616-0.755	< 0.001	0.608	0.705
Napkin ring sign	221	0.671	0.588-0.754	< 0.001	0.582	0.755
Spotty calcification	-	0.505	0.425-0.586	0.893	-	-
Resting						
Plaque with any of high risk features	43	0.658	0.596-0.719	< 0.001	0.497	0.750
Low plaque density	45	0.614	0.542-0.686	0.002	0.476	0.714
Positive remodeling	44	0.691	0.621-0.760	< 0.001	0.570	0.718
Napkin ring sign	45	0.678	0.597-0.758	< 0.001	0.582	0.717
Spotty calcification	-	0.542	0.462 -0.621	0.295	-	-

COV, cut off value; AUC, area under the curve; CI, confidence interval; Sen, sensitivity; Spe, specificity.

Table 7. Incremental value of high hyperemic WSS (hyperemic WSS ≥161) over luminal narrowing for assessing adverse plaque characteristics

Parameters	AUC		Category free NRI		IDI	
	Value	*P*	Value	*P*	Value	*P*
Plaque with any of high risk features						
% DS (reference)*	0.648	< 0.001				
% DS + WSS	0.673	< 0.001	0.406	< 0.001	0.021	0.010
Low plaque density						
% DS (reference) *	0.648	< 0.001				
% DS + WSS	0.659	< 0.001	0.276	0.034	0.005	0.304
Positive remodeling						
% DS (reference) *	0.628	0.001				
% DS + WSS	0.684	< 0.001	0.542	< 0.001	0.039	< 0.001
Napkin ring sign						
% DS (reference) *	0.742	< 0.001				
% DS + WSS	0.763	< 0.001	0.489	0.001	0.017	0.097

Spotty calcification						
% DS (reference) *	0.656	0.001				
% DS + WSS	0.657	< 0.001	-0.068	1.380	0.001	0.658

WSS, wall shear stress; AUC, area under the curve; NRI; net reclassification index; IDI, integrated discrimination index; DS, diameter stenosis.

* Results of % DS were taken as reference values for category free NRI and IDI analyses.

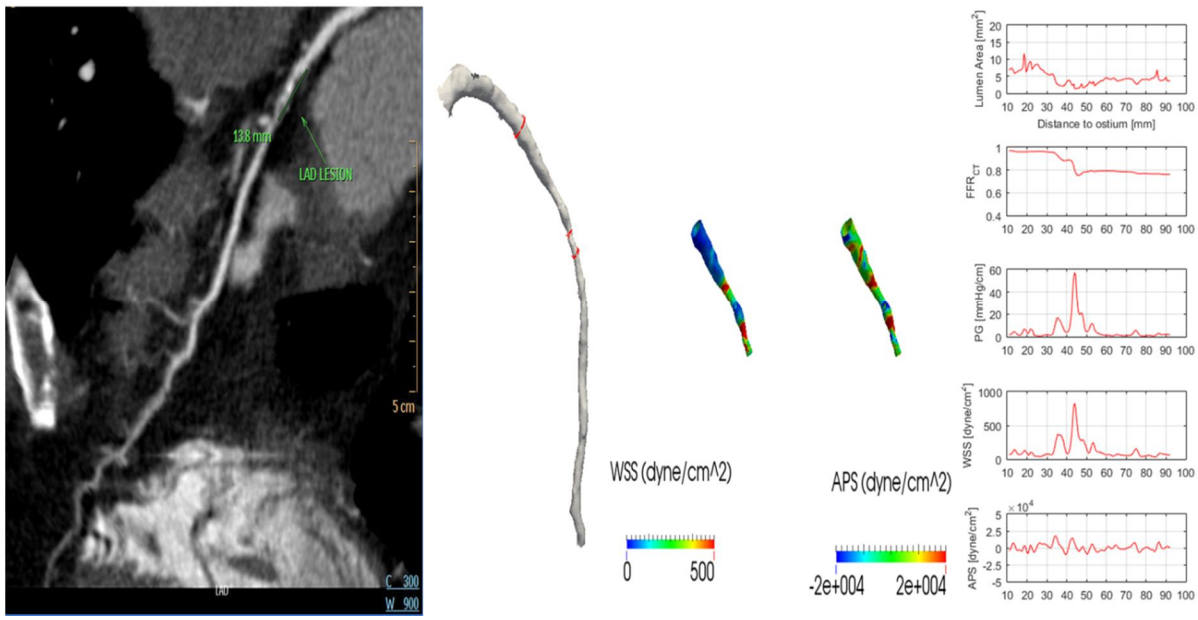

Figure 1. Representative example

(A) The coronary computed tomography angiography demonstrated stenosis in the left anterior descending coronary artery. Coronary computed tomography angiography showed spotty calcification and 41.7% of diameter stenosis.

(B) Average hyperemic WSS was 181 and FFR_{CT} was 0.78.

WSS, wall shear stress; FFR, fractional flow reserve.

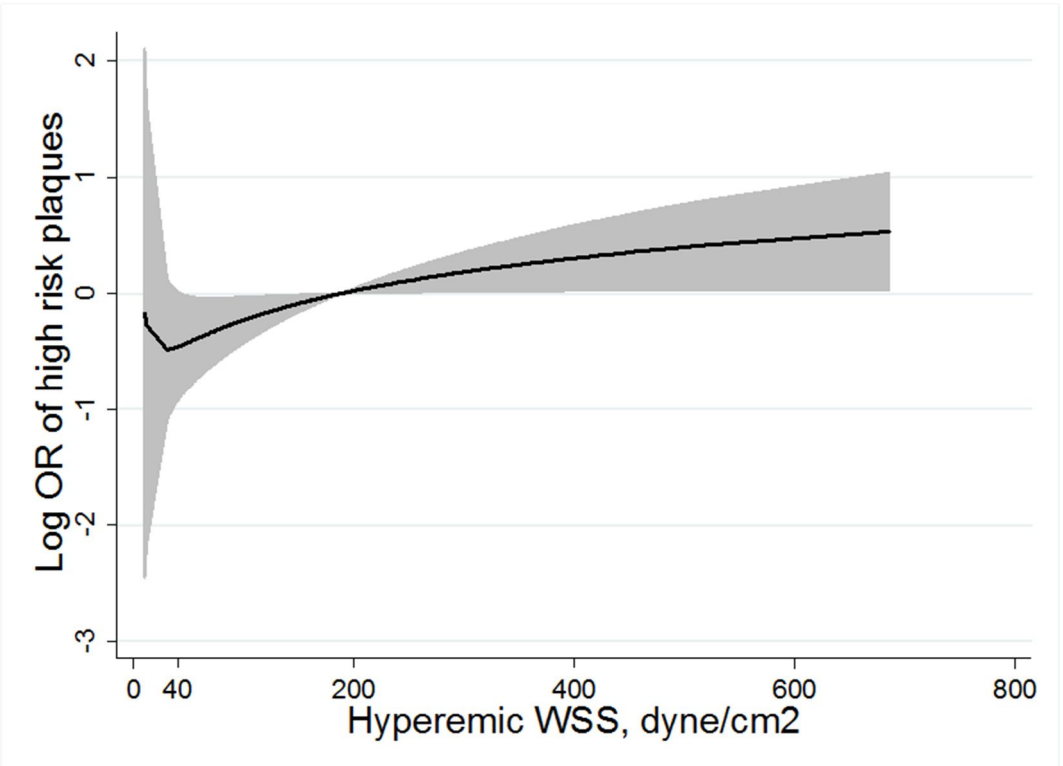

Figure 2. Continuous relation between hyperemic WSS and risk of adverse plaque characteristics calculated by fractional polynomial regression. Gray shading indicates the 95% confidence interval around the flatted line. The OR has been adjusted for the distance from coronary ostium and % diameter stenosis.

WSS, wall shear stress; OR, odds ratio.

Discussion

The major findings of our study are as follows: (1) Plaques exposed to high WSS tend to have poor plaque characteristics; (2) WSS had an incremental value over luminal narrowing in discriminating plaque with any of high risk features; (3) WSS was closely associated with delta pressure, lesion location, MLA and lesion length. These results suggest that CCTA based CFD might be a useful tool for assessing hemodynamic parameters and for predicting plaque rupture. Furthermore, using CFD as a measure of the hemodynamic parameters could improve the risk stratification of coronary artery disease.

Many studies about the contribution of WSS to plaque formation and progression have been published. Mechanical stress is divided into perpendicular and tangential components called tensile stress and shear stress, respectively. The tangential force generated by blood flow induced WSS at the vessel.(4) WSS was calculated by the product of the blood dynamic viscosity and the gradient of the axial velocity at the wall. Because the viscosity of blood vessels cannot change easily, the difference in flow velocity is a determinant factor of WSS.

Some studies have shown that low WSS is involved in early plaque formation and physiological and high WSS are atheroprotective.(15) In response to WSS, endothelial cells produce vasoactive mediator and regulate arterial adaptation.(4, 5) Gnasso *et al.* measured WSS in the carotid arteries of 23 patients.(16) When examining carotid artery by echo Doppler, atherosclerotic involvement of carotid

arteries has lower WSS than in plaque free arteries. In serial quantitative coronary angiography follow up study, there was significant reverse correlation between WSS and atherosclerosis progression.(17)

However, high risk plaques in stenotic lesions under high WSS can be destabilized and high WSS can trigger molecular pathways that weaken the plaques.(15) Recently published systematic review of Slager *et al.* demonstrated that high WSS in the stenotic lesion induce the pathologic progress, thus triggering plaque rupture. In response to high WSS, endothelial cells produce transforming growth factor-β and NO, which suppress smooth muscle proliferation and induce smooth muscle apoptosis. Furthermore, plasmin induced by high WSS increases activity of matrix metalloproteinase, which change related to cap thinning and plaque rupture.(4) Many studies have demonstrated that WSS is important factor of coronary plaque vulnerability.(6, 7) In studies with IVUS among 20 acute coronary syndrome patients showed that all plaque rupture occurred at proximal or top of plaque hill and WSS mapping showed correlation of high WSS sites and plaque rupture sites.(18)

Through the previous conclusions, too low or too high WSS can have a bad effect. Consistent with conclusions, we also found that the OR of APC increased at both extremes of hyperemic WSS.

In a multivariable analysis, higher WSS values are more associated with the lesions that characterized by higher pressure change, more proximal from ostium,

narrower lumen or shorter length. These findings are similar to the earlier studies about patterns of plaque rupture. Previous studies showed that plaque ruptures frequently occurred in proximal part.(19, 20) In IVUS study, plaque rupture parts were mainly in the proximal part of left anterior descending artery and in the proximal and distal part of the right coronary artery. But in left circumflex artery, plaque ruptures were evenly distributed through entire vessel.(19) In our study, multivariable analysis showed that higher WSS was associated with more proximal location in left anterior descending and right coronary artery. But in left circumflex artery, that association was disappeared.

Our study also showed that the addition of WSS to % DS improved the ability to discriminate adverse plaque. Applying WSS values to CCTA stenosis revealed a higher AUC for detection of APC as compared with % DS alone. Furthermore, our study also showed that cut off value of WSS for predicting of APC. The addition of cut off value of WSS to % DS improve the ability to discriminate high risk plaques. Before coronary angiography, luminal narrowing and WSS evaluated by CCTA could improve the risk stratification and provide better effective intervention strategy.

There are several limitations of this study. Because this study is cross-sectional study, causal relationship between WSS and APC is difficult to identify. Second, this model assumed that vessels were rigid and did not reflect blood-vessel interactions. Third, many artifacts such as calcification, patient movement may

affect the clarity of CT. So it is important to follow the exact protocol to get good quality data. Finally, hyperemic condition was not really using adenosine; rather, the hyperemic condition was calculated computationally.

In conclusion, our present study showed that non-invasive CCTA based CFD can be useful in assessing APC. Therefore, hemodynamics of CT derived CFD could improve the risk stratification of coronary artery disease.

References

1. Virmani R, Burke AP, Farb A, Kolodgie FD. Pathology of the vulnerable plaque. *J Am Coll Cardiol.* 2006;47(8 Supplement):C13-C8.
2. Virmani R, Kolodgie FD, Burke AP, Farb A, Schwartz SM. Lessons from sudden coronary death: a comprehensive morphological classification scheme for atherosclerotic lesions. *Arterioscler Thromb Vasc Biol.* 2000;20(5):1262-75.
3. Falk E, Shah PK, Fuster V. Coronary plaque disruption. *Circulation.* 1995;92(3):657-71.
4. Slager CJ, Wentzel JJ, Gijsen FJ, Schuurbiers JC, van der Wal AC, van der Steen AF, Serruys PW. The role of shear stress in the generation of rupture-prone vulnerable plaques. *Nat Clin Pract Cardiovasc Med.* 2005;2(8):401-7.
5. Malek AM, Alper SL, Izumo S. Hemodynamic shear stress and its role in atherosclerosis. *JAMA.* 1999;282(21):2035-42.
6. Park JB, Choi G, Chun EJ, Kim HJ, Park J, Jung JH, Lee MH, Otake H, Doh JH, Nam CW, Shin ES, De Bruyne B, Taylor CA, Koo BK. Computational fluid dynamic measures of wall shear stress are related to coronary lesion characteristics. *Heart.* 2016;102(20):1655-61.
7. Han D, Starikov A, Ó Hartaigh B, Gransar H, Kolli KK, Lee JH, Rizvi A,

Baskaran L, Schulman-Marcus J, Lin FY, Min JK. Relationship Between Endothelial Wall Shear Stress and High-Risk Atherosclerotic Plaque Characteristics for Identification of Coronary Lesions That Cause Ischemia: A Direct Comparison With Fractional Flow Reserve. *J Am Heart Assoc.* 2016;5(12):e004186.

8. Taylor CA, Hughes TJ, Zarins CK. Finite element modeling of three-dimensional pulsatile flow in the abdominal aorta: relevance to atherosclerosis. *Ann Biomed Eng.* 1998;26(6):975-87.
9. Taylor CA, Fonte TA, Min JK. Computational fluid dynamics applied to cardiac computed tomography for noninvasive quantification of fractional flow reserve. *J Am Coll Cardiol.* 2013;61(22):2233-41.
10. Choi G, Lee JM, Kim HJ, Park JB, Sankaran S, Otake H, Doh JH, Nam CW, Shin ES, Taylor CA, Koo BK. Coronary Artery Axial Plaque Stress and its Relationship With Lesion Geometry. *JACC Cardiovasc Imaging.* 2015;8(10):1156-66.
11. Nørgaard BL, Leipsic J, Koo B-K, Zarins CK, Jensen JM, Sand NP, Taylor CA. Coronary computed tomography angiography derived fractional flow reserve and plaque stress. *Curr Cardiovasc Imaging Rep.* 2016;9(1):2.
12. Taylor AJ, Cerqueira M, Hodgson JM, Mark D, Min J, O'Gara P, Rubin

GD; American College of Cardiology Foundation Appropriate Use Criteria Task Force; Society of Cardiovascular Computed Tomography; American College of Radiology; American Heart Association; American Society of Echocardiography; American Society of Nuclear Cardiology; North American Society for Cardiovascular Imaging; Society for Cardiovascular Angiography and Interventions; Society for Cardiovascular Magnetic Resonance. ACCF/SCCT/ACR/AHA/ASE/ASNC/NASCI/SCAI/SCMR 2010 Appropriate Use Criteria for Cardiac Computed Tomography. A Report of the American College of Cardiology Foundation Appropriate Use Criteria Task Force, the Society of Cardiovascular Computed Tomography, the American College of Radiology, the American Heart Association, the American Society of Echocardiography, the American Society of Nuclear Cardiology, the North American Society for Cardiovascular Imaging, the Society for Cardiovascular Angiography and Interventions, and the Society for Cardiovascular Magnetic Resonance. *Circulation.* 2010 Nov 23;122(21):e525-55.

13. Min JK, Taylor CA, Achenbach S, Koo BK, Leipsic J, Nørgaard BL, Pijls NJ, De Bruyne B. Noninvasive Fractional Flow Reserve Derived From Coronary CT Angiography: Clinical Data and Scientific Principles.

JACC Cardiovasc Imaging. 2015;8(10):1209-22.

14. West GB, Brown JH, Enquist BJ. A general model for the origin of allometric scaling laws in biology. *Science.* 1997;276(5309):122-6.
15. Wentzel JJ, Chatzizisis YS, Gijsen FJ, Giannoglou GD, Feldman CL, Stone PH. Endothelial shear stress in the evolution of coronary atherosclerotic plaque and vascular remodelling: current understanding and remaining questions. *Cardiovasc Res.* 2012;96(2):234-43.
16. Gnasso A, Irace C, Carallo C, De Franceschi MS, Motti C, Mattioli PL, Pujia A. In vivo association between low wall shear stress and plaque in subjects with asymmetrical carotid atherosclerosis. *Stroke.* 1997;28(5):993-8.
17. Gibson CM, Díaz L, Kandarpa K, Sacks FM, Pasternak RC, Sandor T, et al. Relation of vessel wall shear stress to atherosclerosis progression in human coronary arteries. Arteriosclerosis, Thrombosis, and Vascular Biology. 1993;13(2):310-5.
18. Fukumoto Y, Hiro T, Fujii T, Hashimoto G, Fujimura T, Yamada J, Okamura T, Matsuzaki M. Localized elevation of shear stress is related to coronary plaque rupture: a 3-dimensional intravascular ultrasound study with in-vivo color mapping of shear stress distribution. *J Am Coll Cardiol.* 2008;51(6):645-50.

19. Hong MK, Mintz GS, Lee CW, Lee BK, Yang TH, Kim YH, Song JM, Han KH, Kang DH, Cheong SS, Song JK, Kim JJ, Park SW, Park SJ. The site of plaque rupture in native coronary arteries: a three-vessel intravascular ultrasound analysis. *J Am Coll Cardiol.* 2005;46(2):261-5.
20. Rodriguez-Granillo GA, García-García HM, Valgimigli M, Vaina S, van Mieghem C, van Geuns RJ, van der Ent M, Regar E, de Jaegere P, van der Giessen W, de Feyter P, Serruys PW. Global characterization of coronary plaque rupture phenotype using three-vessel intravascular ultrasound radiofrequency data analysis. Eur Heart J. 2006;27(16):1921-7.

초 록

서론: 전산 유체 역학은 관상동맥 혈류 역학에 대해 정보를 얻을 수 있는 새로운 비 침습적인 기술이다. 이 논문에서는 전산 유체 역학을 통해 얻은 벽 전단 응력이 유해한 플라크 특성과 관련이 있는지 많은 수에서 밝히고자 하였다.

방법: 관상동맥 전산화 단층 촬영을 시행한 143명의 대상에서 296개의 병변을 후향적으로 등록하였다. 전산 유체 역학 분석을 통해 관상 동맥 혈류, 압력, 길이에 따른 압력 하강 (압력 차), 전산화 단층 촬영에서 확인한 fractional flow reserve와 벽 전단 응력 등의 혈역학적 지표를 구했다. 유해한 플라크의 특성은 low density plaque, positive remodeling, napkin ring sign, spotty calcification 으로 정의되었고, 최소 내강 영역에서 평가되었다.

결과: 유해한 플라크의 특성 중 하나라도 가지는 플라크는 296개 병변 중 147개 (49.7%) 에서 확인되었고, 그 중 가장 흔한 특성은 low density plaque 였다 (n = 82, 27.7%). 벽 전단 응력을 3분위 수로 나누어 가장 높은 벽 전단 응력에 노출된 군에서 유해한 플라크의 특성을 나타내는 빈도가 높은 것을 확인하였다. Receiver operating characteristic curve를 통해서 확인한 유해한 플라크의 특성을 예측하

는 벽 전단 응력의 cut off value는 161이었다. 직경 협착에 대해 높은 벽 전단 응력 (hyperemic WSS ≥ 161 dyne/cm^2) 을 추가하였을 때 유해한 플라크를 확인, 재분류 하는데 도움이 되는 것을 확인하였다. (area under the curves: 0.648 to 0.673, P < 0.001; category free net reclassification index 0.406, P < 0.001; integrated discrimination index 0.021, P = 0.010). Spotty calcification을 제외한 유해한 플라크의 특성에 대해 벽 전단 응력을 추가하는 것이 유해한 플라크를 확인, 재분류 하는 데에 도움이 되는 것을 확인하였다.

결론: 컴퓨터 단층 촬영에 의해 계산된 전산 유체 역학은 비침습적인 기술로 불리한 플라크의 특성을 발견하고, 이는 나아가 관상 동맥 질환에 대한 환자의 위험 층화에 도움이 될 수 있을 것으로 보인다.

주요어: 벽 전단 응력, 전산 유체 역학, 플라크, 관상 동맥 질환, 관상 동맥 전산화 단층 촬영

학번: 2016-21910